Effect of Hemopexin Treatment on Outcome after Intracerebral Hemorrhage in Mice

Jing Chen-Roetling[a,1], **Yang Li**[b], **Yang Cao**[a], **Zhe Yan**[a], **Xiangping Lu**[a], **Raymond F. Regan**[a,b,*]

[a]Department of Emergency Medicine, Thomas Jefferson University, 1025 Walnut Street, Philadelphia, PA 19107

[b]Department of Emergency Medicine, University of Maryland School of Medicine, 110 S. Paca Street, 6th Floor, Suite 200, Baltimore, Maryland 21205 USA (Present Address)

Abstract

Heme release from hemoglobin may contribute to secondary injury after intracerebral hemorrhage (ICH). The primary endogenous defense against heme toxicity is hemopexin, a 57 kDa glycoprotein that is depleted in the CNS after hemorrhagic stroke. We hypothesized that systemic administration of exogenous hemopexin would reduce perihematomal injury and improve outcome after experimental ICH. Intraperitoneal treatment with purified human plasma hemopexin beginning 2 hours after striatal ICH induction and repeated daily for the following two days reduced blood-brain barrier disruption and cell death at 3 days. However, it had no effect on neurological deficits at 4 or 7 days or striatal cell viability at 8 days. Continuous daily hemopexin administration had no effect on striatal heme content at 3 or 7 days, and did not attenuate neurological deficits, inflammatory cell infiltration, or perihematomal cell viability at 8 days. These results suggest that systemic hemopexin treatment reduces early injury after ICH, but this effect is not sustained, perhaps due to an imbalance between striatal tissue heme and hemopexin content at later time points. Future studies should investigate its effect when administered by methods that more efficiently target CNS delivery.

Keywords

Heme; hemoglobin toxicity; iron; stroke; stroke models, subararachnoid hemorrhage

1. Introduction

Intracerebral hemorrhage (ICH) deposits millimolar concentrations of heme into the brain parenchyma. While initially sheltered in the hydrophobic pockets of hemoglobin within intact erythrocytes, erythrolysis begins within a few hours and progresses over the following days to weeks (Liu et al., 2019). Extracellular hemoglobin rapidly autoxidizes to methemoglobin, a process that greatly diminishes the affinity of heme for its globin chains (Kassa et al., 2016). Transfer of highly reactive heme moieties to membrane protein and lipid binding sites has adverse effects on adjacent cells. Direct toxicity is produced by multiple mechanisms including indiscriminate oxidation of lipids, proteins and DNA, disruption of cation gradients, and membrane destabilization via a colloid-osmotic mechanism (Kumar and Bandyopadhyay, 2005). Heme breakdown by the heme oxygenase enzymes releases iron, which if not rapidly deposited into ferritin can further contribute to oxidative stress by catalyzing lipid peroxidation by the Fenton reaction (Sadrzadeh et al., 1984). A growing body of experimental evidence indicates that iron-mediated accumulation of cell lipid hydroperoxides may lead to cell death in perihematomal tissue by ferroptosis, a regulated process that is inhibited by the activity of glutathione peroxidase 4 (Bai et al., 2020; Zhang et al., 2018; Zille et al., 2017). Primary heme or iron toxicity may be further compounded by a secondary inflammatory response that is initiated at least in part by activation of toll-like receptors-2 or -4 by heme (Figueiredo et al., 2007; Sansing et al., 2011).

Hemopexin (Hpx) is ~57 KDa glycoprotein that tightly binds heme (affinity constant $1.9 \times 10^{14} \times M^{-1}$(Hrkal et al., 1974)), effectively removing heme/hemin from accessible binding sites and preventing its participation in free radical reactions. In concert with haptoglobin, it provides the primary defense against circulating heme associated with sickle cell disease and other hemolytic states (Smith and McCulloh, 2015). In cortical cell cultures, overexpression of Hpx by adenoviral gene transfer reduced oxidative injury markers and apoptotic cell death due to blood clot co-culture (Liu et al., 2020). Consistent with these observations, Leclerc et al. reported that increasing brain hemopexin using an adeno-associated vector prior to experimental ICH decreased lesion volumes and neurological deficits (Leclerc et al., 2016), thereby identifying hemopexin as a potential therapy for ICH.

The hemopexin concentration in the healthy CNS is very low at baseline (~5 μg/ml in CSF (Roher et al., 2009)) and is negligible after hemorrhagic stroke (Righy et al., 2018), providing little heme binding capacity. However, rapid blood-brain barrier breakdown after ICH may provide perihematomal tissue with access to circulating hemopexin. In support of this hypothesis, we have reported that mice lacking hemopexin sustained more injury and had worse functional outcomes in striatal collagenase and blood injection ICH models (Chen et al., 2011). It remains to be determined if increasing circulating Hpx to supraphysiologic concentrations would provide a further level of protection. The aim of the present study was to assess the therapeutic relevance of systemic Hpx therapy after experimental ICH. Toward that end, we conducted a preclinical trial of plasma Hpx treatment using established mouse collagenase and blood injection ICH models.

2. Results

2.1. Hemopexin dosing.

Initial dosing was guided by prior use of human Hpx i.p. in a mouse model (Rolla et al., 2013). Commercial ELISA assays that specifically detected human or mouse Hpx without species cross-reactivity were used to quantify serum levels. A single 70 mg/kg dose produced a human serum Hpx concentration of 0.87 ± 0.03 mg/ml at 2 hours (Fig. 1). In contrast, the baseline mouse serum Hpx concentration was 0.49 ± 0.11 mg/ml. Repeated administration at 24-hour intervals for a total of 3 doses was sufficient to maintain a human serum Hpx concentration of 0.65–1.26 mg/ml throughout the 96-hour observation period. Surprisingly, the initial human Hpx injection produced a transient increase in mouse Hpx that had resolved by 26 hours and did not recur with subsequent human Hpx injections.

2.2. Hemopexin injection reduces blood-brain barrier injury.

Consistent with prior observations, parenchymal collagenase injection produced blood-brain barrier disruption that was readily detected by fluorescent assay of Evans blue leakage into the striata of vehicle-treated mice (Fig. 2A). This signal was reduced by approximately 40% in mice receiving 70 mg/kg Hpx at 2 hours after collagenase and repeated once daily for a total of 3 doses.

2.3. Effect of hemopexin injection on striatal cell viability.

In mice injected with parenchymal collagenase followed by vehicle i.p. at 2 hours and then daily for 3 total doses, striatal cell viability was approximately half of that of contralateral striata at 3 days. It was significantly increased in mice receiving 3 doses of 70 mg/kg Hpx (Fig. 2B). At a lower dose (35 mg/kg), Hpx had no effect in the collagenase model (viability $55.2\pm3.5\%$ v. $59.2\pm4.8\%$ in vehicle group), but did provide significant protection in the blood injection model (viability $84.3\pm4.0\%$ v. $66.0\pm2.1\%$ in vehicle group). Treatment with 70 mg/kg of heme-saturated Hpx for 3 daily doses was ineffective (Fig. 2C). The protective effect of 70 mg/kg heme-free hemopexin was lost when the observation period was extended to 8 days (Fig. 2D).

2.4. Hemopexin (3 doses) had no effect on activity level or other behavioral deficits.

Digital analysis of 30 minute video recordings of mice in their standard cage environment demonstrated no baseline differences between vehicle and Hpx-treated groups in total activity time, defined as seconds spent feeding, hanging, jumping, rearing, and walking (Fig. 3A). Activity was reduced at 4 and 7 days after collagenase-induced ICH in both groups, but Hpx treatment (70 mg/kg $\times$ 3 daily doses) had no effect. There were likewise no differences in adhesive removal, elevated body swing or corner tests (Fig 3B–D).

2.5. Hemopexin treatment had no effect on striatal heme content.

On day 3 after collagenase-induced ICH, ipsilateral striatal heme content, consisting of all heme including that bound to Hb, was 101.64 ± 8.04 nmoles in vehicle-treated mice (n = 9 mice) and 98.48 ± 7.89 nmoles in mice receiving 3 daily doses of 70 mg/kg Hpx (n=8, P = 0.78 v. vehicle). At day 7, striatal heme content was likewise very similar in mice treated

daily with vehicle (32.96±5.79 nmoles, n = 10 mice) and Hpx (31.38±4.68 nmoles, P = 0.83, n=10 mice).

The tissue concentration of injected human Hpx was subsequently investigated. In collagenase-injected striata at 2 hours after the first Hpx dose, human Hpx content was 1.83 ± 0.25 pmoles, compared with 0.04 ± 0.01 pmoles in control mice injected with human Hpx but without collagenase-induced hemorrhage (n = 6 mice/group).

2.6. Effect of continuous Hpx treatment.

We hypothesized that continued daily treatment with Hpx 70 mg/kg until termination of the experiment would provide sustained benefit. The blood injection ICH model was used for these experiments. As observed with the collagenase model, overall cage activity was reduced by striatal autologous blood injection and recovered over the following week at a similar rate in Hpx and vehicle groups (Fig. 4A). Mean neurological deficit scores tended to be lower in Hpx-treated mice, suggesting improved function, but did not differ significantly when adjusted for multiple comparisons (Fig. 4B). Results of corner and adhesive removal tests were also similar between Hpx and vehicle groups (Fig. 4 C,D). At the conclusion of behavioral testing, no differences in striatal cell viability were detected in mice treated Hpx (70.8±6.1% v. contralateral striata) and vehicle (69.8±4.3%).

Systemic Hpx treatment has previously been shown to inhibit inflammatory cell migration (Spiller et al., 2011). We therefore quantified neutrophils and microglia/macrophages in injected and contralateral striata. Mean inflammatory cell numbers did not significantly differ between vehicle and Hpx groups at 3 and 7 days (Fig. 5).

2.7. Mortality.

A total of six of the 270 mice used in this study died before completion of the experiment. Four of these mice were in vehicle group and two were in the Hpx group.

3. Discussion

These results provide novel information about the efficacy of systemic Hpx therapy after experimental ICH. Intraperitoneal Hpx initiated 2 hours after ICH at a dose sufficient to increase total serum Hpx by up to 3.5-fold had an early protective effect, as quantified by blood-brain barrier integrity and perihematomal cell viability at 3 days. Unfortunately this benefit was not sustained. Neurological deficits, perihematomal cell viability at 8 days, and striatal inflammatory cell number did not differ between Hpx and vehicle control groups despite continuing daily Hpx injections. These observations suggest that Hpx may have some therapeutic potential for ICH, but systemic administration per se is inadequate.

An inherent limitation of i.p Hpx administration is its CNS bioavailability relative to the heme content of a hematoma. An experimental hemorrhage volume of 25 microliters contains approximately 250 nanomoles of heme. In contrast, the tissue human Hpx content in hemorrhagic striata at two hours after i.p. injection of 70 mg/kg, the higher dose used in this study, was only ~2 picomoles. At early time points after hemorrhage, most heme is still sequestered within erythrocytes, and low concentrations of any leaked hemoglobin or

heme will be scavenged in part by endogenous haptoglobin and Hpx. The additional albeit modest delivery of exogenous Hpx to perihematomal tissue observed in this study may then be sufficient to provide some benefit when endogenous Hpx binding sites are saturated. However, this low Hpx level would be expected to have little effect as erythrolysis becomes widespread, which has been observed at about 3 days in rodent models (Jaremko et al., 2010; Wagner and Dwyer, 2004; Xi et al., 1998).

Hpx is generally considered a cytoprotective protein, but toxicity has also been reported, which may be mediated by its protease activity and by paradoxical pro-inflammatory and pro-oxidant effects observed in vitro (Bakker et al., 2005; Bakker et al., 2010; Chen-Roetling et al., 2018). The relevance of these mechanisms to acute cell injury in vivo has not been established and remains controversial (Mauk et al., 2011). Late toxicity that negates any early benefit of Hpx therapy is unlikely in the present series of experiments due to the weak striatal delivery of administered Hpx. However, it cannot be excluded, and should be considered in the design of further studies that use alternate methods to produce higher perihematomal tissue levels.

Hpx has been previously reported to inhibit inflammatory cell migration in a sepsis model, possibly due in part to its protease activity rather than heme binding (Spiller et al., 2011). We hypothesized that systemic Hpx administration would reduce infiltration of neutrophils and microglia/macrophages into perihematomal tissue, with potential therapeutic benefit. However, stereology-guided cell counts demonstrated no significant difference in striatal neutrophil or microglia/macrophage numbers at either 3 or 7 days after ICH despite continuous daily Hpx dosing. These results suggest that the effect of Hpx on inflammatory cell chemotaxis in sepsis may be less relevant after hemorrhagic stroke.

The present study was made possible by a supply of purified human hemopexin provided as a gift by CSL Behring, Inc. Mouse Hpx has limited availability, and the cost of commercially-available mouse or human Hpx would otherwise have been prohibitive at the doses administered. However, the use of human Hpx in a mouse injury model is a limitation of this study. Human Hpx has been tested in multiple mouse injury models to date with therapeutic effects (Belcher et al., 2018; Graw et al., 2016; Rolla et al., 2013), and the early benefit observed in the present study is consistent with these observations. Both rodent and human Hpx bind protein-free heme with high affinity, but cellular uptake of Hpx-heme complexes may have some species-specificity, which may have reduced subsequent heme clearance (Taketani et al., 1998). Furthermore, it is possible that an immune response antagonized the efficacy of human Hpx that was administered at later time points. These issues should be addressed in future studies using species-specific Hpx.

The present results do not exclude a sustained benefit of Hpx therapy if administered by a method that increases its CNS bioavailability in a timely fashion. Intranasal therapies, for example, are easily initiated in the prehospital and emergency department settings. In rodents, this route can produce micromolar cortical or striatal drug concentrations within 30 minutes (Hanson et al., 2009). Intranasal administration has been used in ICH models to test the efficacy of a variety of proteins, small molecules, and stem cells, with largely positive results (Chen-Roetling and Regan, 2019). Alternatively, Hpx could be continuously infused

directly into the hematoma, peri-hematomal tissue or an adjacent ventricle. However, in a clinical setting, initiation of a CNS infusion would likely be delayed for the several hours needed for mobilization of specialized personnel and facilities. Preclinical studies should therefore be designed to test its efficacy when treatment is delayed for several hours after hemorrhage. A combined approach using early intranasal or systemic administration followed within hours by direct CNS infusion may be most effective at rapid and sustained delivery of therapeutic quantities of Hpx, and seems worthy of further investigation in ICH models.

4. Experimental Procedure

4.1. Animals.

All procedures were conducted in accordance with protocols approved by the Institutional Animal Care and Use Committee (IACUC) at Thomas Jefferson University, where all procedures involving animals were performed. This work was conducted in accordance with EC Directive 86/609/EEC and uniform requirements for manuscripts submitted to biomedical journals. Swiss-Webster mice (8–12 weeks old, males and females) were obtained from Taconic Laboratories. Mice were housed exclusively in the Thomas Jefferson University animal facility, which is fully accredited by the Association for Assessment and Accreditation of Laboratory Animal Care International. Food and water were available ad libitum, and mice were kept under a 12-hour light/darkness cycle. Mice were acclimated for at least one week in this facility prior to initiation of all experiments. Control and experimental groups for all endpoints contained balanced numbers of males and females.

4.2. ICH induction.

Right striatal ICH was produced by stereotactic injection of sterile collagenase (Sigma-Aldrich C9572) or autologous blood following previously described methods (Chen-Roetling et al., 2019). Inhalation anesthesia was achieved with 2% isoflurane in oxygen; rectal temperature was continuously monitored and maintained at 37±0.5°C. After aseptic preparation of the surgical site, a scalp incision was made, and a burr hole was drilled at the following coordinates relative to bregma: 2.5 mm lateral, 0.5 mm anterior. A 28–30 g Hamilton needle was then inserted 3 mm below the skull surface and 0.028–0.060 units collagenase was injected in a sterile artificial CSF solution (NaCl 148 mmol/l, KCl 3 mmol/l, CaCl2 1 mmol/l, MgCl2, 0.8 mmol/l, Na2HPO4 0.8 mmol/l, NaH2PO4 0.2 mmol/l). Due to some variability in potency of different collagenase lots, the dose required to reduce striatal cell viability by approximately 40–60% at 4 days after injection was used. All direct comparisons were made between mice receiving the same collagenase dose. The previously described procedure to minimize loss of collagenase activity during dilution was rigorously followed (Chen-Roetling et al., 2013). Alternatively, mice were injected with 25 μl autologous blood obtained from a tail vessel, collected in a sterile citrated Eppendorf tube, and injected at 1 μl/minute. Surgical control mice were subjected to anesthesia and needle insertion only.

4.3. Hemopexin injection.

Random assignment of mice to treatment groups was guided by an online random number generator (www.random.org). Sterile human plasma Hpx (CSL Behring, King of Prussia, PA, USA) was used exclusively in all experiments. It was administered by intraperitoneal (i.p.) injection beginning 2 hours after striatal collagenase or blood injection and was repeated daily for 3–7 doses. Control mice were injected with sterile PBS vehicle only.

Outcome Measures were conducted at prespecified time points that were optimized for the collagenase or blood injection ICH models while minimizing animal usage, as follows:

4.4. Hemopexin assays.

Blood was obtained from a tail vein at prespecified time points after Hpx injection and allowed to clot. Assays were conducted using ELISA kits specific for human and mouse Hpx (Innovative Research, Inc., Novi, MI USA, Cat. No. IRKTAH2562 and Life Diagnostics, Inc., West Chester, PA, USA, Cat No. HPX-1, respectively), following manufacturer's instructions. For tissue assays, striata were collected in 500 µl lysis buffer (210 mM mannitol, 70 mM sucrose, 5 mM HEPES, 1 mM EDTA, 0.1% sodium dodecyl sulfate, and 0.1% Triton X-100) and stored at −70°C until used.

4.5. Cell viability assay.

Methylthiazolyldiphenyl-tetrazolium (MTT) assay was performed on freshly-dissociated striatal tissue as previously described (Chen-Roetling et al., 2019). Mice were euthanized under deep isoflurane anesthesia by cervical dislocation. Brains were removed, and injected and contralateral striata were dissected free and placed in separate tubes containing 1 ml Hanks Balanced Salt Solution supplemented with 27.5 mM glucose, 20.5 mM sucrose and 4.2 mM sodium bicarbonate. Tissue was then dissociated to provide all cells with uniform and rapid MTT access, using a standard trituration technique. MTT was then added (final concentration 0.125 mg/ml) and tubes were placed into a water bath (37°C) for 4 minutes. After low speed centrifugation, supernatant was removed and the formazan product was extracted in 2 ml isopropanol (91%). Absorbance (562 nm) was quantified, and signals from injected striata were normalized to those from contralateral striata (= 100). Prior studies have validated this method when compared with cell counts of histological sections or fluorescence measurements of striatal homogenates in mice expressing the red fluorescent protein dTomato specifically in central neurons (Chen-Roetling et al., 2013; Chen-Roetling et al., 2017; Qu et al., 2007).

4.6. Blood-brain barrier permeability assay.

As previously detailed (Chen-Roetling et al., 2019), mice received 4 ml/kg i.p. of sterile 2% Evans blue in saline. After a 3 hour circulation interval, they were perfused under 2% isoflurane anesthesia with 25 ml sterile saline injected into the left ventricle to flush out intravascular Evans blue. Injected and contralateral striata were then removed and placed into separate tubes. Tissue was then treated with 50% trichloroacetic acid (Uyama et al., 1988), the supernatant was collected, and its fluorescence (ex:620 nm, em:680 nm) was quantified. The fluorescence signal in contralateral striata was subtracted from that in hemorrhagic striata to calculate the signal specific to ICH injury.

4.7. Histology.

After anesthesia with isoflurane, mice were perfused via left ventricular cardiac injection with 5–7 ml isotonic saline and then 20 ml of 4% paraformaldehyde, followed by postfixation in 4% paraformaldehyde for 7 hours at 4°C. Brains were then placed into 0.1 M phosphate buffer (pH 7.4) containing 20% sucrose and stored at 4°C; the sucrose solution was replaced after 12 hours. Tissue sectioning and immunostaining were performed by FD Neurotechnologies, Columbia MD, USA, using: 1) Anti-Iba1, Wako Chemicals USA, Richmond, VA,USA, Cat. No. 019–19741, 1:10,000; 2) Anti-myeloperoxidase, Dako, Santa Clara, CA, USA; Cat.No. A0398, 1:10,000. Cell counts of were performed by a researcher blinded to experimental groups using the Stereologer system (SRC Biosciences, Tampa, FL, USA), as previously described in detail.(Chen-Roetling et al., 2013; West, 1993)

4.8. Behavioral testing.

All observations were performed by a researcher blinded to treatment groups, following prespecified and established protocols as follows:

A. Spontaneous motor activity was quantified by digital analysis of video recordings as previously described (Chen et al., 2011). Video recording was conducted in a room maintained at 72±4°F, using cameras mounted perpendicular to the long axis of each cage. Videos were analyzed using HomeCageScan (CleverSys, Inc., Reston VA, USA), quantifying time spent feeding, hanging, jumping, rearing, and walking. Total time in these activities was summed to provide an index of motor activity.

B. Adhesive removal test: Adhesive dots (3 mm) were placed on the right or left forepaw, and removal time was recorded. The time needed for removal of the adhesive from the right forepaw (ipsilateral to the lesion) was subtracted from that of the left forepaw to yield the asymmetry score (MacLellan et al., 2006).

C. Elevated body swing test: The mouse was held by the tester approximately 3 cm from the base of its tail, and lifted 3 cm above the surface. Left and right swings were observed for 45 seconds, and the percentage left swings was then quantified. A right striatal lesion induces a tendency to swing to the left (Liu et al., 2008).

D. Corner test: Two boards were attached at one end at a 30 degree angle. As the mouse explored the corner, upward rearing and turning were observed. A mouse with a right striatal lesion prefers to turn to the right. The percentage right turns for 6 trials was recorded (Zhang et al., 2002).

E. Neurological deficit score was calculated following the method of Glusahakov et al.(Glushakov et al., 2013), assessing abnormalities in circling behavior, limb and body symmetry, and gait.

4.9. Heme assay.

Striata were removed at indicated time points and dissociated in 500 μl formic acid. After centrifugation (17,000 × g, 30 min) the supernatant was collected and absorbance (398 nm)

was quantified and compared to that of a hemin standard curve prepared in formic acid with nonhemorrhagic striatal tissue lysate. The absorbance of the sample from the contralateral uninjected striatum was subtracted to obtain the signal specific for the ICH.

4.10. Statistics.

Data were analyzed using GraphPad Prism 8.0.2. Differences in experiments using 3 or more treatment groups were via one-way ANOVA and the Bonferroni multiple comparisons test. Experiments with 2 treatment groups used unpaired t-test.

Time lines of experiments are provided in Fig. 6.

Acknowledgements:

References

Bai Q, Liu J, Wang G, 2020. Ferroptosis, a Regulated Neuronal Cell Death Type After Intracerebral Hemorrhage. Front Cell Neurosci. 14, 591874. [PubMed: 33304242]

Bakker WW, Borghuis T, Harmsen MC, van den Berg A, Kema IP, Niezen KE, Kapojos JJ, 2005. Protease activity of plasma hemopexin. Kidney International. 68, 603–10. [PubMed: 16014037]

Bakker WW, Melgert BN, Faas MM, 2010. Hemopexin: anti-inflammatory, pro-inflammatory, or both? Journal of Leukocyte Biology. 87, 1–2; author reply 3, 5. [PubMed: 20047881]

Belcher JD, Chen C, Nguyen J, Abdulla F, Zhang P, Nguyen H, Nguyen P, Killeen T, Miescher SM, Brinkman N, Nath KA, Steer CJ, Vercellotti GM, 2018. Haptoglobin and hemopexin inhibit vaso-occlusion and inflammation in murine sickle cell disease: Role of heme oxygenase-1 induction. PLoS One. 13, e0196455. [PubMed: 29694434]

Chen-Roetling J, Lu X, Regan KA, Regan RF, 2013. A rapid fluorescent method to quantify neuronal loss after experimental intracerebral hemorrhage. J Neurosci Methods. 216, 128–36. [PubMed: 23583700]

Chen-Roetling J, Kamalapathy P, Cao Y, Song W, Schipper HM, Regan RF, 2017. Astrocyte heme oxygenase-1 reduces mortality and improves outcome after collagenase-induced intracerebral hemorrhage. Neurobiol Dis. 102, 140–146. [PubMed: 28323022]

Chen-Roetling J, Ma SK, Cao Y, Shah A, Regan RF, 2018. Hemopexin increases the neurotoxicity of hemoglobin when haptoglobin is absent. Journal of Neurochemistry. 145, 464–473. [PubMed: 29500821]

Chen-Roetling J, Cao Y, Peng D, Regan RF, 2019. Rapid Loss of Perihematomal Cell Viability in the Collagenase Intracerebral Hemorrhage Model. Brain Research.

Chen-Roetling J, Regan RF, 2019. Intranasal drug delivery after intracerebral hemorrhage. In Therapeutic Intranasal Delivery for Stroke and Neurological Disorders. Springer Series in Translational Stroke Research, Vol., Chen J, Wang J, Wei L, Zhang J, ed.^eds. Springer, Cham, Switzerland, pp. 43–55.

Chen L, Zhang X, Chen-Roetling J, Regan RF, 2011. Increased striatal injury and behavioral deficits after intracerebral hemorrhage in hemopexin knockout mice. J Neurosurg. 114, 1159–67. [PubMed: 21128737]

Figueiredo RT, Fernandez PL, Mourao-Sa DS, Porto BN, Dutra FF, Alves LS, Oliveira MF, Oliveira PL, Graca-Souza AV, Bozza MT, 2007. Characterization of heme as activator of Toll-like receptor 4. J Biol Chem. 282, 20221–9. [PubMed: 17502383]

Glushakov AV, Robbins SW, Bracy CL, Narumiya S, Dore S, 2013. Prostaglandin F2alpha FP receptor antagonist improves outcomes after experimental traumatic brain injury. J Neuroinflammation. 10, 132. [PubMed: 24172576]

Graw JA, Mayeur C, Rosales I, Liu Y, Sabbisetti VS, Riley FE, Rechester O, Malhotra R, Warren HS, Colvin RB, Bonventre JV, Bloch DB, Zapol WM, 2016. Haptoglobin or Hemopexin Therapy Prevents Acute Adverse Effects of Resuscitation After Prolonged Storage of Red Cells. Circulation. 134, 945–60. [PubMed: 27515135]

Hanson LR, Roeytenberg A, Martinez PM, Coppes VG, Sweet DC, Rao RJ, Marti DL, Hoekman JD, Matthews RB, Frey WH 2nd, Panter SS, 2009. Intranasal deferoxamine provides increased brain exposure and significant protection in rat ischemic stroke. J Pharmacol Exp Ther. 330, 679–86. [PubMed: 19509317]

Hrkal Z, Vodrazka Z, Kalousek I, 1974. Transfer of heme from ferrihemoglobin and ferrihemoglobin isolated chains to hemopexin. Eur J Biochem. 43, 73–8. [PubMed: 4209590]

Jaremko KM, Chen-Roetling J, Chen L, Regan RF, 2010. Accelerated Hemolysis and Neurotoxicity in Neuron-Glia-Blood Clot Co-cultures. J Neurochem. 114, 1063–73. [PubMed: 20497302]

Kassa T, Jana S, Meng F, Alayash AI, 2016. Differential heme release from various hemoglobin redox states and the upregulation of cellular heme oxygenase-1. FEBS Open Bio. 6, 876–84.

Kumar S, Bandyopadhyay U, 2005. Free heme toxicity and its detoxification systems in human. Toxicology Letters. 157, 175–88. [PubMed: 15917143]

Leclerc JL, Santiago-Moreno J, Dang A, Lampert AS, Cruz PE, Rosario AM, Golde TE, Dore S, 2016. Increased brain hemopexin levels improve outcomes after intracerebral hemorrhage. J Cereb Blood Flow Metab. 271678X16679170.

Liu DZ, Cheng XY, Ander BP, Xu H, Davis RR, Gregg JP, Sharp FR, 2008. Src kinase inhibition decreases thrombin-induced injury and cell cycle re-entry in striatal neurons. Neurobiol Dis. 30, 201–11. [PubMed: 18343677]

Liu R, Li H, Hua Y, Keep RF, Xiao J, Xi G, Huang Y, 2019. Early Hemolysis Within Human Intracerebral Hematomas: an MRI Study. Transl Stroke Res. 10, 52–56. [PubMed: 29766451]

Liu Y, Tan C, Li W, Liu X, Wang X, Gui Y, Qin L, Deng F, Hu C, Chen L, 2020. Adenoviral transfer of hemopexin gene attenuates oxidative stress and apoptosis in cultured primary cortical neuron cell exposed to blood clot. Neuroreport. 31, 1065–1071. [PubMed: 32804709]

MacLellan CL, Auriat AM, McGie SC, Yan RH, Huynh HD, De Butte MF, Colbourne F, 2006. Gauging recovery after hemorrhagic stroke in rats: implications for cytoprotection studies. J Cereb Blood Flow Metab. 26, 1031–42. [PubMed: 16395282]

Mauk MR, Smith A, Mauk AG, 2011. An alternative view of the proposed alternative activities of hemopexin. Protein Science. 20, 791–805. [PubMed: 21404362]

Qu Y, Chen-Roetling J, Benvenisti-Zarom L, Regan RF, 2007. Attenuation of oxidative injury after induction of experimental intracerebral hemorrhage in heme oxygenase-2 knockout mice. J Neurosurg. 106, 428–35. [PubMed: 17367065]

Righy C, Turon R, Freitas G, Japiassu AM, Faria Neto HCC, Bozza M, Oliveira MF, Bozza FA, 2018. Hemoglobin metabolism by-products are associated with an inflammatory response in patients with hemorrhagic stroke. Rev Bras Ter Intensiva. 30, 21–27. [PubMed: 29742229]

Roher AE, Maarouf CL, Sue LI, Hu Y, Wilson J, Beach TG, 2009. Proteomics-derived cerebrospinal fluid markers of autopsy-confirmed Alzheimer's disease. Biomarkers. 14, 493–501. [PubMed: 19863188]

Rolla S, Ingoglia G, Bardina V, Silengo L, Altruda F, Novelli F, Tolosano E, 2013. Acute-phase protein hemopexin is a negative regulator of Th17 response and experimental autoimmune encephalomyelitis development. J Immunol. 191, 5451–9. [PubMed: 24154625]

Sadrzadeh SMH, Graf E, Panter SS, Hallaway PE, Eaton JW, 1984. Hemoglobin: A biologic Fenton reagent. J. Biol. Chem 259, 14354–56. [PubMed: 6094553]

Sansing LH, Harris TH, Welsh FA, Kasner SE, Hunter CA, Kariko K, 2011. Toll-like receptor 4 contributes to poor outcome after intracerebral hemorrhage. Ann Neurol. 70, 646–56. [PubMed: 22028224]

Smith A, McCulloh RJ, 2015. Hemopexin and haptoglobin: allies against heme toxicity from hemoglobin not contenders. Front Physiol. 6, 187. [PubMed: 26175690]

Spiller F, Costa C, Souto FO, Vinchi F, Mestriner FL, Laure HJ, Alves-Filho JC, Freitas A, Rosa JC, Ferreira SH, Altruda F, Hirsch E, Greene LJ, Tolosano E, Cunha FQ, 2011. Inhibition of neutrophil

migration by hemopexin leads to increased mortality due to sepsis in mice. Am J Respir Crit Care Med. 183, 922–31. [PubMed: 20971829]

Taketani S, Immenschuh S, Go S, Sinclair PR, Stockert RJ, Liem HH, Muller Eberhard U, 1998. Hemopexin from four species inhibits the association of heme with cultured hepatoma cells or primary rat hepatocytes exhibiting a small number of species specific hemopexin receptors. Hepatology. 27, 808–14. [PubMed: 9500711]

Uyama O, Okamura N, Yanase M, Narita M, Kawabata K, Sugita M, 1988. Quantitative evaluation of vascular permeability in the gerbil brain after transient ischemia using Evans blue fluorescence. J Cereb Blood Flow Metab. 8, 282–4. [PubMed: 3343300]

Wagner KR, Dwyer BE, 2004. Hematoma removal, heme, and heme oxygenase following hemorrhagic stroke. Ann NY Acad Sci. 1012, 237–251. [PubMed: 15105270]

West MJ, 1993. New stereological methods for counting neurons. Neurobiol Aging. 14, 275–85. [PubMed: 8367009]

Xi GH, Keep RF, Hoff JT, 1998. Erythrocytes and delayed brain edema formation following intracerebral hemorrhage in rats. J. Neurosurg 89, 991–996. [PubMed: 9833826]

Zhang L, Schallert T, Zhang ZG, Jiang Q, Arniego P, Li Q, Lu M, Chopp M, 2002. A test for detecting long-term sensorimotor dysfunction in the mouse after focal cerebral ischemia. J Neurosci Methods. 117, 207–14. [PubMed: 12100987]

Zhang Z, Wu Y, Yuan S, Zhang P, Zhang J, Li H, Li X, Shen H, Wang Z, Chen G, 2018. Glutathione peroxidase 4 participates in secondary brain injury through mediating ferroptosis in a rat model of intracerebral hemorrhage. Brain Research. 1701, 112–125. [PubMed: 30205109]

Zille M, Karuppagounder SS, Chen Y, Gough PJ, Bertin J, Finger J, Milner TA, Jonas EA, Ratan RR, 2017. Neuronal Death After Hemorrhagic Stroke In Vitro and In Vivo Shares Features of Ferroptosis and Necroptosis. Stroke. 48, 1033–1043. [PubMed: 28250197]

Highlights

- Intraperitoneal hemopexin reduced blood-brain barrier injury at 3 days after ICH.

- It also reduced perihematomal cell loss at 3 days but not at 8 days.

- Hemopexin treatment had no effect on neurological deficits or tissue heme content.

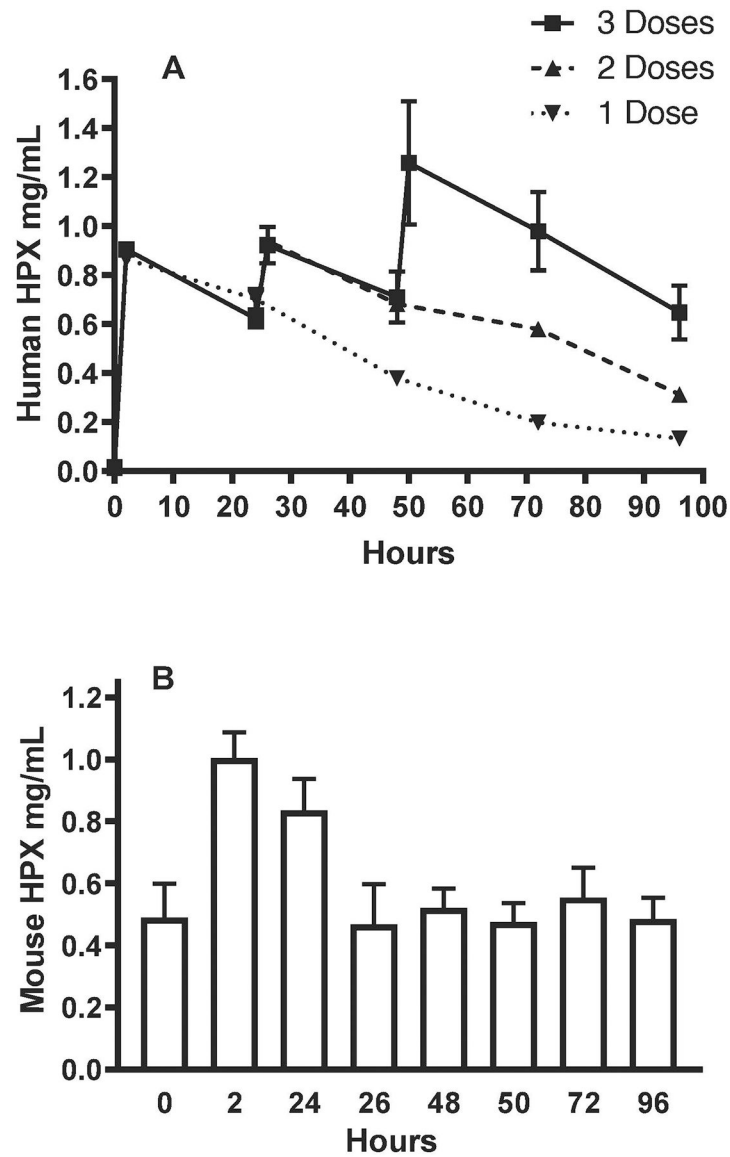- Systemic hemopexin therapy per se provides only transient protection after ICH.

Figure 1.
Effect of human hemopexin (Hpx) injections on serum Hpx concentrations. A) Mice were injected with 70 mg/kg human Hpx i.p. as a single dose (0 hour), or with two or three doses separated by 24-hour intervals (0 hour, 24 hours, 48 hours). Blood was collected from a tail vein for human Hpx immunoassay at baseline and at 2h, 24h (before second dose), 26h, 48h (before third dose), 50h, 72h and 96h. B) Same serum samples as in A were tested for mouse Hpx (mean ± S.E.M., 4–8 mice/condition).
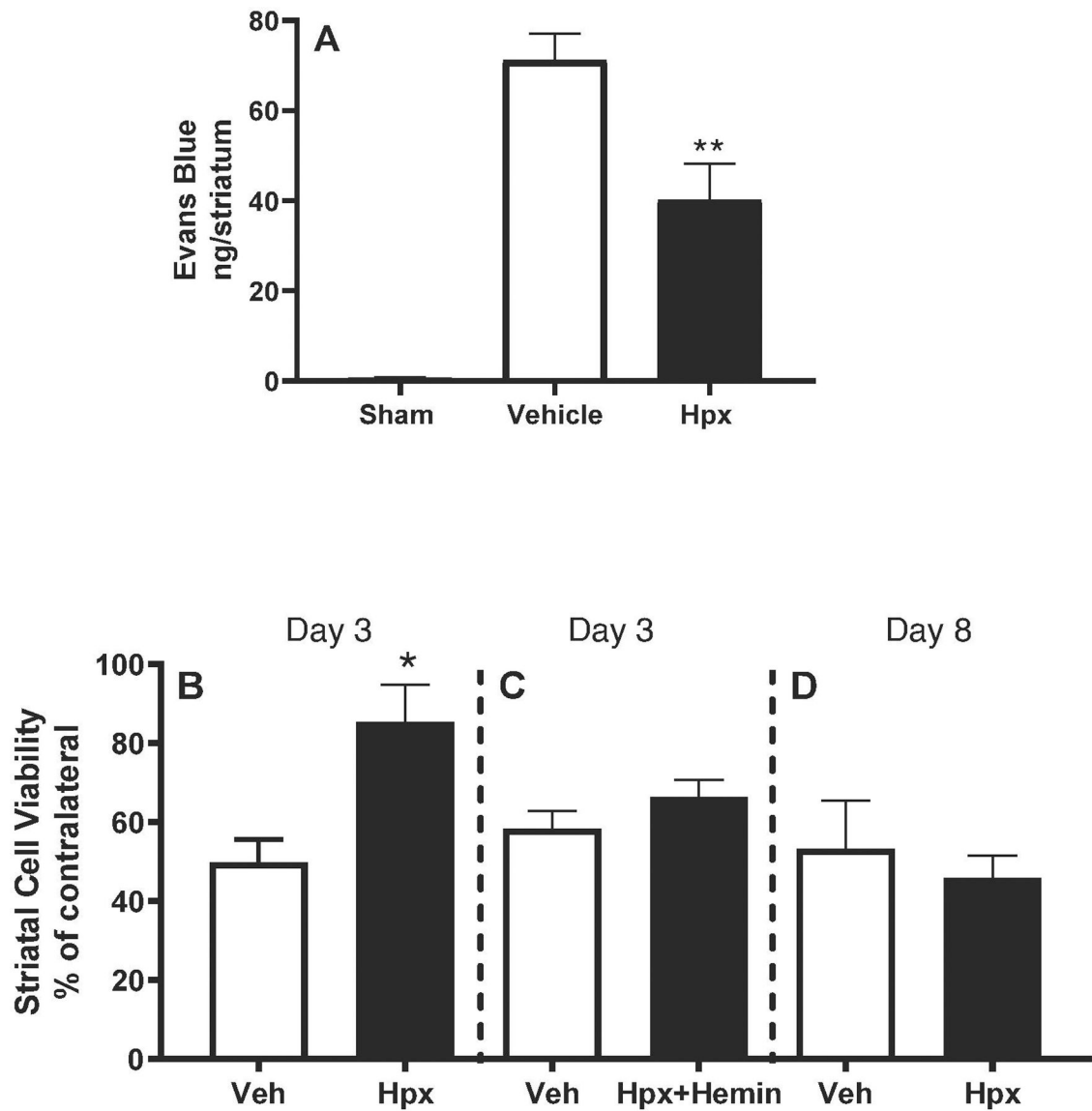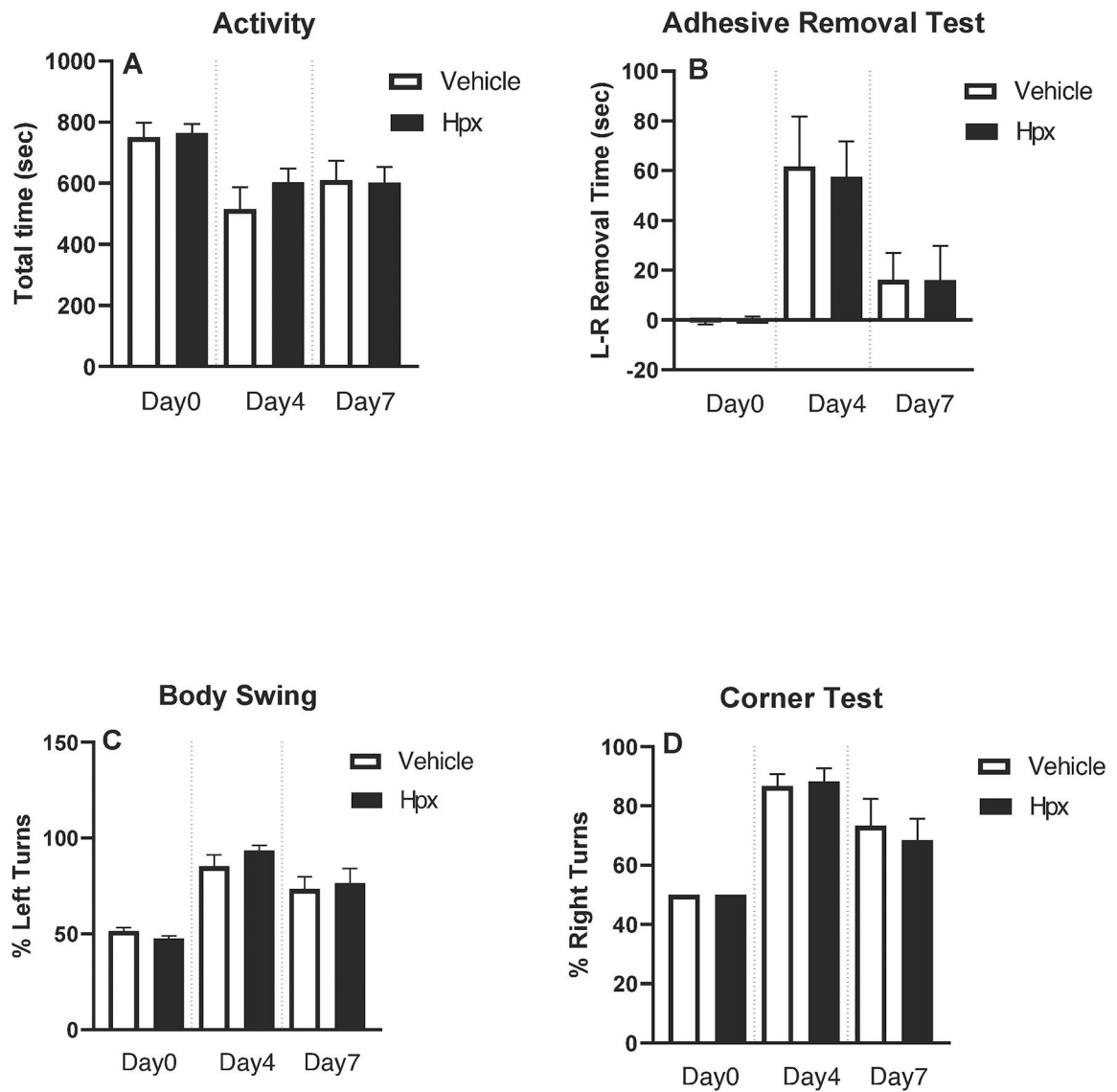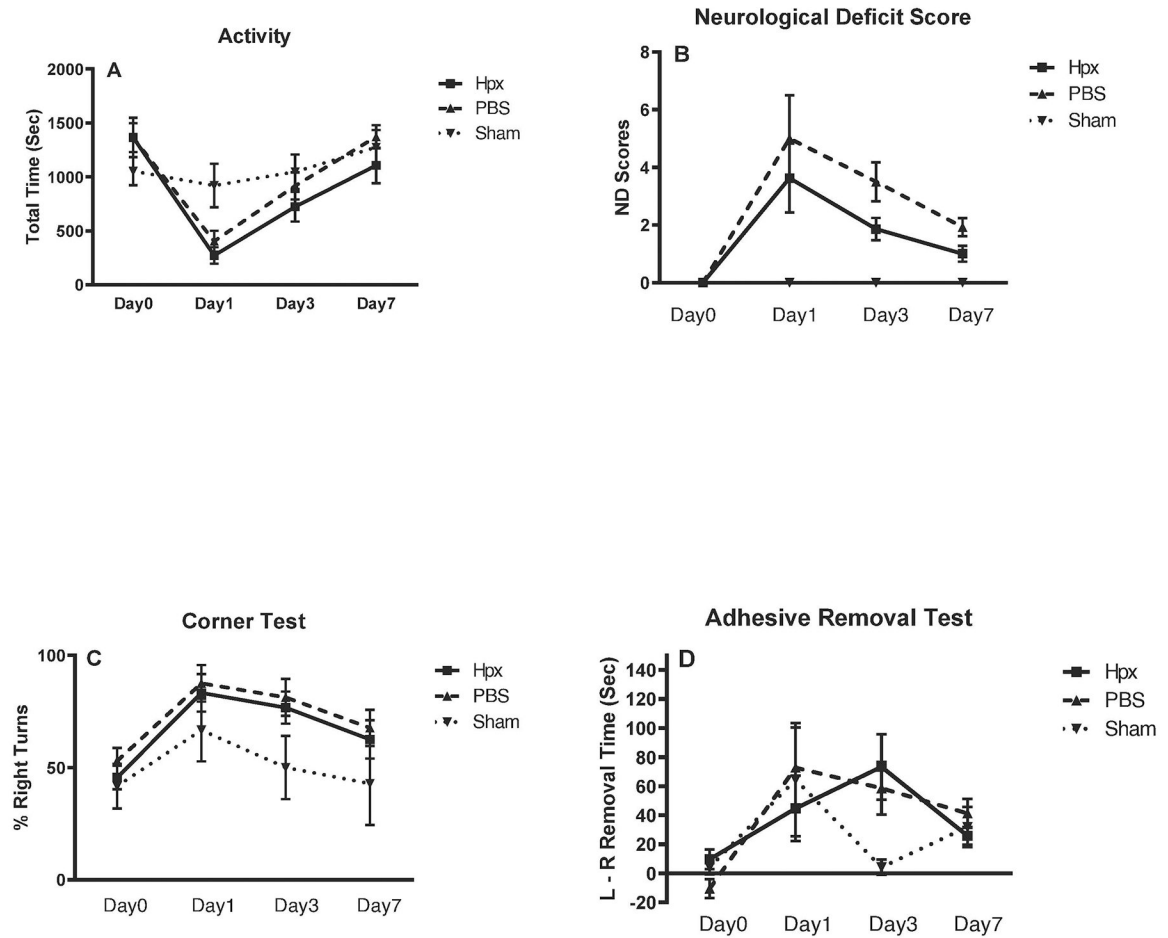
Figure 2.

Early protective effect of hemopexin therapy. Right striatal ICH was induced in mice with collagenase, followed 2 hours later by 70 mg/kg Hpx i.p., 70 mg/kg Hpx with equimolar hemin, or PBS vehicle (Veh); treatments were repeated 24 and 48 hours later. A) Right striatal blood-brain barrier permeability was quantified on Day 3 by Evans blue assay (mean ± S.E.M, n=7/condition for treatment groups and 5/condition for sham); B) Right striatal cell viability at 3 days was quantified by MTT conversion for foramazan, normalized to the contralateral striatum (=100, n = 5/condition); C) Mice were treated with vehicle or heme-saturated Hpx (n = 14/condition); D) Mice were treated with 70 mg/kg Hpx for 3 doses as in A; cell viability was assessed on Day 8 (n = 10/condition). *P < 0.05, **P < 0.01 v. corresponding vehicle condition.

Figure 3.
Hemopexin treatment (3 doses) had no effect on behavioral outcome. Neurological deficits were assessed at 4 and 7 days after collagenase-induced ICH by: (A) digital quantification of motor activity during 30 minute video while in standard mouse cage; (B) adhesive removal test; (C) elevated body swing test; (D) corner test. Bars represent mean ± S.E.M., n = 10/condition.

Figure 4.
Effect of daily hemopexin treatment (total 7 doses) on behavioral outcome. ICH was induced by right striatal autologous blood injection, followed at 2 hours by 70 mg/kg Hpx or vehicle i.p., repeated at 24 hour intervals for 7 days. Neurological deficits were assessed at indicated time points by: (A) home cage motor activity quantification (60 minute video); (B) neurological deficit score; (C) corner test; (D) adhesive removal test. Each point represents mean ± S.E.M., 7–17 mice/condition for treatment groups and 5–8 mice/condition for sham groups.
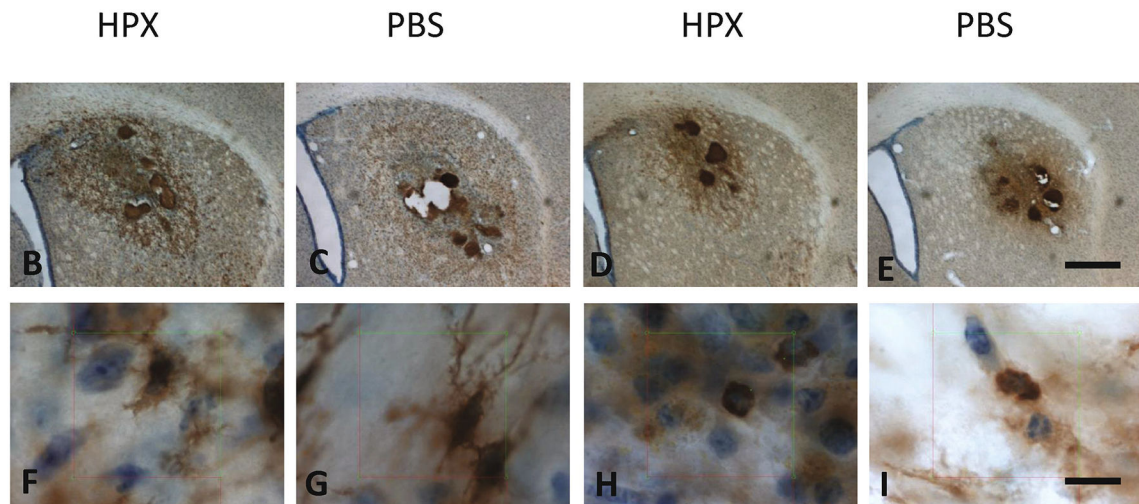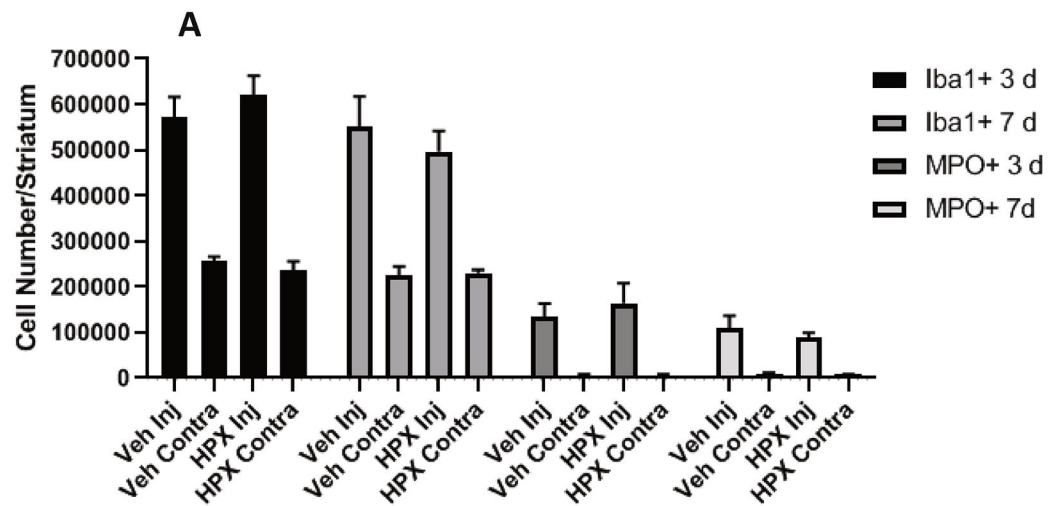
Figure 5.

Hemopexin treatment has no effect on striatal inflammatory cell numbers after ICH. A) Number of Iba1 and myeloperoxidase positive cells in hemorrhagic (Injected, Inj) and contralateral (Contra) striata at indicated time points after hemorrhage induction in mice (6–8/condition) treated with hemopexin 70 mg/kg or vehicle. Hemopexin treatment began at 2 hours and was repeated at 24 hour intervals until completion of the experiment. B-I) Representative photos captured from stereology counting session of sections from mice at 7 days after striatal blood injection, immunostained with anti-Iba1 (B,C,F,G)or myeloperoxidase (MPO, D,E,H,I). Scale bars 500 μm B-E, 10 μm F-I).
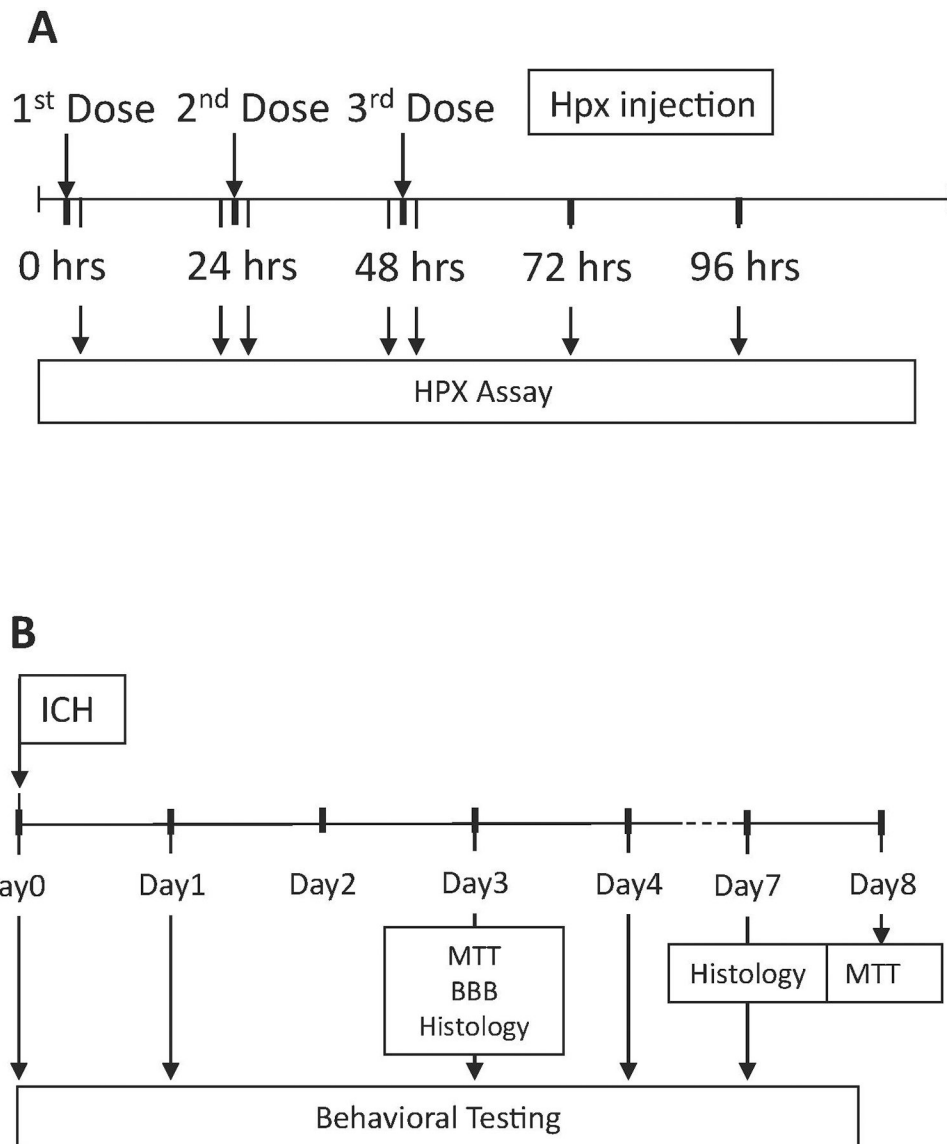
Figure 6.
Timeline of experiments testing: A) effect of Hpx treatment on human and mouse serum Hpx levels; B) effect of Hpx treatment on striatal cell viability (MTT assay), blood-brain barrier (BBB) disruption (Evans blue assay), histology and behavioral deficits after ICH.